Thermogravimetric and Resistivity Study of *Ex Situ* and *In Situ* Poly(methyl methacrylate)/Carboxylic Acid Group Functionalized Multiwall Carbon Nanotubes Composites

Mahuya Das,[1]* Dipa Ray,[2] Sri Bandyopadhyay,[3] Sourish Banerjee,[4] Nil R. Bandyopadhyay,[1] Amitava Basumallik[5]

[1]*School of Material Science & Engineering, Bengal Engineering & Science University, Shibpur, Howrah 711 103, West Bengal, India*
[2]*Department of Polymer Science & Technology, Calcutta University, 92, A.P.C. Road, Kolkata 700009, West Bengal, India*
[3]*School of Materials Science & Engineering, University of New South Wales, Sydney 2052, Australia*
[4]*Department of Physics, Calcutta University, 92, A.P.C. Road, Kolkata 700009, West Bengal, India*
[5]*Metallurgy and Materials Engineering, Bengal Engineering & Science University, Shibpur, Howrah 711 103, West Bengal, India*

Received 7 February 2009; accepted 29 August 2010
DOI 10.1002/app.33320
Published online 12 January 2011 in Wiley Online Library (wileyonlinelibrary.com).

ABSTRACT: Polymer composites based on poly(methyl methacrylate) (PMMA)/carboxylic acid group functionalized multiwall carbon nanotubes (MWCNT) were prepared by the *ex situ* and *in situ* techniques with 0.05% loading by weight. Composite films were fabricated by solvent casting method. Electrical conductivity of the composites as well as of the neat PMMA polymer was measured in the temperature range 333 K to 423 K. Neat PMMA samples prepared by the same method showed complete insulating behavior. *Ex situ* technique leads to a lower value of percolation threshold. Infrared spectroscopy was used to analyze the effect of functionalization of MWCNT on the interfacial bonding of PMMA and MWCNT. Thermogravimetric analysis revealed that the maximum degradation temperature has been shifted to higher region for *in situ* composites compared to PMMA itself—and the *ex situ* composites indicated better thermal stability. X-ray diffraction study of composites also indicates that *in situ* composites functionalization incorporated MWCNT particles in the polymer chain. © 2011 Wiley Periodicals, Inc. J Appl Polym Sci 120: 2954–2961, 2011

Key words: nanocomposites; dispersions; FTIR; thermogravimetric analysis (TGA); X-ray

INTRODUCTION

The strength, flexibility, unique dimensions, unusual current conduction capacity, etc of carbon nanotubes (CNT) make them valuable for potential use in controlling other nanoscale structures with variable application, which suggests they will have an important role in nanotechnology applications. A number of authors have reported using CNT as nanoreinforcing agent in polymeric matrix, and the researchers characterized the composited with respect to their mechanical, thermal, electrical, and dynamical mechanical properties.[1–4]

There are reports based on poly(methyl methacrylate) (PMMA) as the matrix. Costache et al.[5] studied thermal degradation of PMMA and its nanocomposites to determine the effect of clays (anionic and cationic) or CNT on the degradation pathway and the degradation of the nanocomposite occurred at higher temperatures. Yuen et al. prepared multiwall CNT (MWCNT)/PMMA composites by *in situ* and *ex situ* methods. Standard error of the mean microphotographs reveal that the MWCNT/PMMA composites that are prepared *in situ* adhere better than those prepared *ex situ*. MWCNT/PMMA composites prepared *in situ* exhibit a lower electrical resistivity and a lower percolation threshold than those prepared *ex situ*. The effects of the method of processing the MWCNT/PMMA, the MWCNT content, and the composite stacking process on the shielding effectiveness (SE) of the electromagnetic interference of the MWCNT/PMMA composites were examined. The SE of electromagnetic interference of MWCNT/PMMA increased with MWCNT content. The composites prepared *in situ* have higher SE values. Additionally, composites prepared by stacking 10 layers of 0.1 mm MWCNT/PMMA have a higher SE than that prepared from a single 1.0-mm thick piece of bulk MWCNT/PMMA. The characteristic SE spectra of all systems were also discussed.

**Present address:* JIS College of Engineering, Kalyani, Nadia-741235, West Bengal, India.
Correspondence to: M. Das (d_mahuya@yahoo.com).

Du et al.[7] developed a new processing method to produce PMMA/single-wall carbon nanotubes (SWCNT) composites, which was claimed to provide better dispersion of SWCNT in the polymer matrix. Optical microscopy of the samples showed improved dispersion of SWCNT in the PMMA matrix, which is a key factor of the composite performance.

Ivanov et al.[8] carried out electrospinning of stable solutions of SWCNT and polymers (including thermosets and biocompatible polymers such as PMMA, poly ethylene oxide, poly vinyl alcohol, poly vinyl acetate, poly carbonate) to produce composite fibers with diameters varying from a few nanometers to hundreds of microns. High degrees of alignment of SWCNT along the axis of the fibers were achieved as characterized by polarized microRaman spectroscopy of the SWCNT within the fiber (up to 18 : 1 intensity ratio) for fibers with diameter less than ~20 μ. The strain-induced shift of the 2600 cm^{-1} Raman band of the single-wall nanotubes (SWNT) inside the composites was used to investigate the load transfer to the nanotubes during their controlled mechanical loading.

Sundaray et al.[9] produced conducting nanocomposite fibers of MWCNT/PMMA by electrospinning. The fibers obtained this way were long and well aligned. The CNT were found to be oriented along the fiber axis. Room temperature dc electrical conductivity of a single fiber with MWCNT (0.05% w/w) showed ~10 orders of magnitude improvement over the pure PMMA. The conductivity increased with MWCNT concentration.

It is thus obvious that there is a continued need to find out the most efficient way to utilize such amazing nanomaterial properly for newer applications by innovative techniques. In spite of its great potential, the fundamental problem of dispersion of CNT in polymeric matrix still exists which disturbs the effective use of polymer/CNT nanocomposites. It is caused by CNT insolubility in organic solvents, or in polymers, together with strong Van der Waals interaction between individual tubes with tendency to agglomerate. In fact CNT is produced in the form of bundles or bundle aggregations consisting of 50 to a few hundred individual CNT, or in CNT ropes, or as a network from individual CNT (SWCNT), MWCNT.[10] Consequently, polymer composites prepared by mixing in polymer melt or polymer solution possess different states of tube dispersion. Direct mixing of CNT into polymer melt is modified with high power dispersion methods, such as application of ultrasound and high speed shearing. Other techniques include the use of surfactants during blending with polymer latex,[11] surfactants for *in situ* polymerization,[11–13] polymerization from the surface of CNT,[14] or chemical modification of CNT, for example, by end and defect-site chemistry or covalent sidewall functionalization of CNT.[15,16]

In this work, —COOH group functionalized MWCNT is used for more efficient dispersion of CNT in the polymeric matrix to enhance the interfacial adhesion in the composites. The aim of the work is to study, the effectiveness of functionalization along with the used *ex situ* and *in situ* technique to improve the electrical conductivity of an otherwise totally insulating polymer such as PMMA i.e., to generate a low cost semiconducting polymer.

EXPERIMENTAL

Materials

PMMA, supplied by Himedia Chemicals (M_w 25000) was used as the polymer matrix. Isobutyl methyl ketone (IBMK) (Merck) with analytical purity was used as solvent, and benzoyl peroxide (Merck) as the initiator. The MWCNT functionalized with carboxylic acid group, purified, were supplied by Cheap Tube with diameter 10–30 nm, length 1–10 mm. Nanocomposites were fabricated with 0.05 weight % loading of MWCNT by two different technique: i) *in situ* and ii) *ex situ* techniques.

Fabrication of composites

In situ technique

MWCNT were sonicated first in IBMK for 2 h. Then MMA monomer (which was made inhibitor free and vacuum distilled previously) was added to the dispersion of MWCNT and further sonicated for 1 h. Initiator (0.5% of total weight of MMA) was then added to the total solution. Polymerization was carried out at 60°C (maintained by heating in a water bath) under magnetic stirring for 2 h. PMMA/MWCNT polymer films were prepared by casting of the prepared polymer composite solution and dried. The typical thickness of the films was ~0.5 mm.

Ex situ technique

MWCNT were sonicated first in IBMK for 2 h. Then PMMA polymer was added to the dispersion of MWCNT and further sonicated for 3 h. PMMA/MWCNT polymer films were prepared by casting of the prepared polymer composite solution and drying. The typical thickness of the films was ~0.5 mm.

TESTING

Electrical resistivity measurements

Electrical resistivity for —COOH functionalized MWCNT loaded PMMA composite system was studied in the temperature range 333 K to 423 K. Samples were cut in suitable dimension for loading

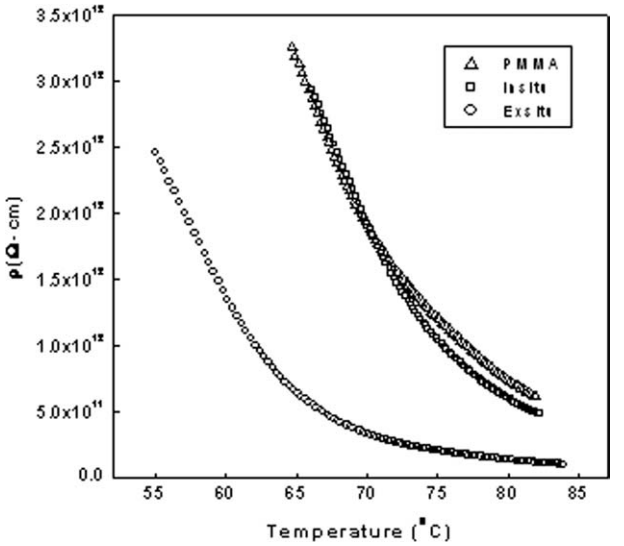

Figure 1 Plot of resistivity versus temperature for PMMA resin and composites samples.

in the sample holder. Typical area of the sample surface was ~1.0 cm^2 and thickness ~0.5 mm. Silver paste was painted on opposite surfaces and the samples were baked at ~323 K for a few minutes to adhere the paste on the surfaces. The samples were loaded in a vacuum chamber with vacuum level ~10^{-3} mbar. Electrical resistance of the samples was measured by two-probe method using Keithley 6514 System Electrometer. Temperature of the samples was monitored by Eurotherm 3216 Temperature controller with ± 0.1°C accuracy. Temperature versus resistance data was recorded using standard interfacing software.

XRD analysis

All samples were characterized by X-ray diffraction (XRD) using Philips "X-pert Pro" diffraction unit attached with secondary monochromator, automatic divergence slit and nickel filter which had a CuKα radiation source operated at a generator voltage, 45 kV and current, 40 μA.

FTIR analysis

The chemical structure of PMMA/MWCNT composites was characterized by a Fourier transform infrared spectrometer (FTIR-8400, Shimadzu).

Thermogravimetric analysis

The samples were subjected to differential thermal analysis (DTA)/thermogravimetric analysis (TGA) studies at a flow of 20 mL/min nitrogen using Diamond TGA/DTA analytical instrument at a heating rate of 5°C/min.

RESULTS AND DISCUSSIONS

Resistivity study

Resistivity data (Fig. 1) show that neat PMMA and *in situ* PMMA nanocomposite have almost the same resistivity level over the temperature range 50°C–85°C. *Ex situ* composites show lower resistivity than the resin and the *in situ* composite.

The activation energies are also very similar as seen in Figure 2. The values of activation energy for pure PMMA is 0.99 ± 0.002 eV and for 0.05% (by weight) *in situ* CNT doped sample it is 1.194 ± 0.003 eV. The error in activation energy is very small indicating that the resistivity variation is governed by the single activation energy over the temperature. Also, the *ex situ* interface states have different activation energy compared to the matrix. Near linear nature of the curves indicates that the resistivity is controlled by some activated process with the activation energy E_a given by the following formula

$$\rho = \rho_0 \exp(E_a/K_B T)$$

where ρ is the corresponding resistivity at temperature T expressed in Kelvin; ρ_0 is the pre-exponential resistivity factor in the limit $T \rightarrow \infty$ and K_B is the Boltzmann constant. From Figure 2, it can be seen that there are two regions of conduction with different activation energies for the *ex situ* doped PMMA/MWCNT composites. Resistivity data shows a clear signature of two activation energies 1.346 eV and 0.851 eV below and >70°C respectively. The change from one region to the other is not sharp but is gradual. The activation energy in the higher temperature range is lower than that in the lower temperature range. The increase in E_a is observed at certain temperatures depending on the composition. The values

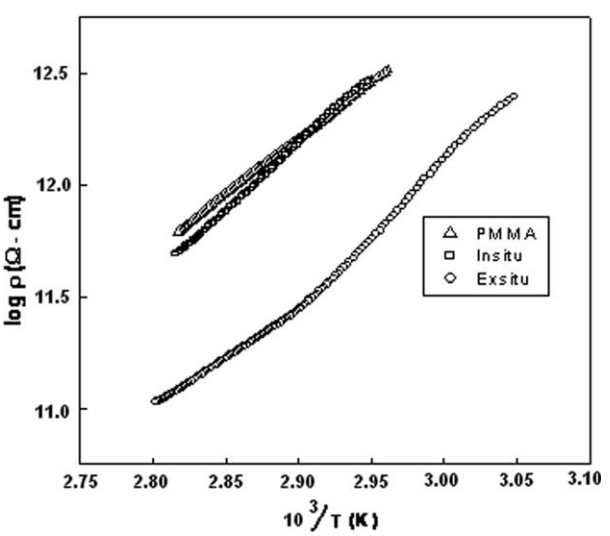

Figure 2 Plot of logρ versus 1/T for PMMA resin and nanocomposite samples.

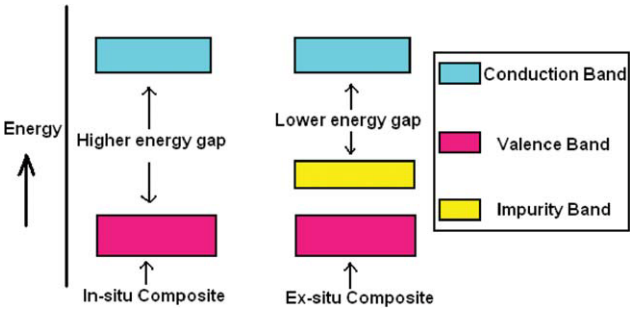

Figure 3 Energy diagram for *in situ* composite and *ex situ* composites. [Color figure can be viewed in the online issue, which is available at wileyonlinelibrary.com.]

of these temperature at which E_a is increased, is determined from the intersection of the linear parts drawn for each conduction region.

Resistivity data indicates that MWCNT has a decisive role in controlling the charge transport mechanism in the present polymer system. In case of semiconductor, the lowering of resistivity or increase in conductivity is obvious with increase in temperature due to the excitation of more number of electron in valence band, which reduces the band gap between the valence band and conduction band (Fig. 3). This is evident from the resistivity curve (Fig. 1) in the case of the *in situ* composite. However, the fact that the value of resistivity of *in situ* composite is still high (more or less similar to that of the insulator PMMA) even with incorporation of MWCNT may be attributed to a) the presence of —COOH group, and b) the MWCNT was incorporated in the polymer chain during polymerization, hence showing similar electrical properties like PMMA.

The overall resistivity of the *ex situ* composite consists of the high temperature intrinsic and low temperature extrinsic regions. The intrinsic region is due to the band-to-band electron transport in polymer MWCNT composite system. In the *ex situ* nanocomposites, perhaps due to the dispersion technique, the MWCNT did not get a chance to be incorporated into the polymer chains so intimately; rather it was most likely distributed along the polymer grains in a homogeneous manner with a distinct mean free path between them.[17] The resulting interface has higher conductivity by a factor of 6 compared to the bulk polymer and also the *in situ* nanocomposite.

MWCNT for *ex situ* composites particles also introduces large amount of localized impurity states within the composite. These states are distributed randomly in positional coordinate and energy scale. This state creates an impurity band between the valence band and the conduction band (Fig. 3). Electron hopping results between these states, with minimum energy expenditure i.e., activation energy for excitation of electron will be reduced. This is consistent with the three orders of magnitude reduction of the low temperature activation energy compared with the other sample as evident from Figure 2. It is clear from the graph that in the low temperature region thermal energy of the order of tens of meV controls the electron hopping between the defect states.

It is apparent that in this study, at higher temperature by *ex situ* technique an otherwise completely insulating material like PMMA exhibits semiconducting nature which may be more pronounced with increase in loading of MWCNT. It is worth noting in the reported literature that in PMMA/MWCNT nanocomposite obtained by electrospinning the CNTs was found to be oriented along the fiber axis. The room temperature dc electrical conductivity of a single fiber with MWCNT (0.05% w/w) showed some 10 orders of magnitude improvement over pure PMMA.[9] Similar orders of increase in conductivity have been reported by Luechinger et al.[17] in graphene coated cobalt nanoparticles reinforced PMMA.

Infrared study

Figure 4 shows the infrared (IR) spectra of MMA monomer which is characterized by peaks at 1749 cm^{-1} (C=O carboxyl group for ester), 1637 cm^{-1} (C=C double bond) and within 1100–1200 cm^{-1} (C—O stretching).

Figure 5 presents the IR spectra of PMMA resin and —COOH functionalized CNT. For PMMA, IR peaks observed were at 1748 cm^{-1} (C=O carboxyl group for ester), 1637 cm^{-1} (C=C double bond, weaker than the MMA monomer) and within 1100–1200 cm^{-1} (C—O stretching). C—H stretching peak at 2952 cm^{-1} has become weaker in case of PMMA due to polymerization. In the IR spectra of MWCNT, peaks at 1720 cm^{-1} (C=O carboxyl group for —COOH group), and 1639.81 cm^{-1} (C=C double bond) are present.

The feature near 1760 cm^{-1} is attributed to the COO- bonds and indicates that COO- functional

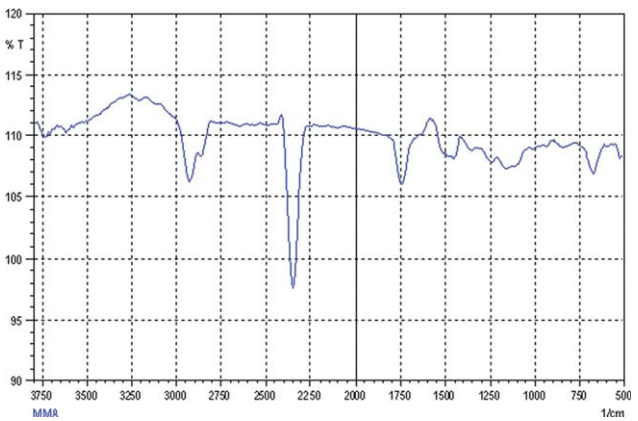

Figure 4 IR spectra of MMA monomer. [Color figure can be viewed in the online issue, which is available at wileyonlinelibrary.com.]

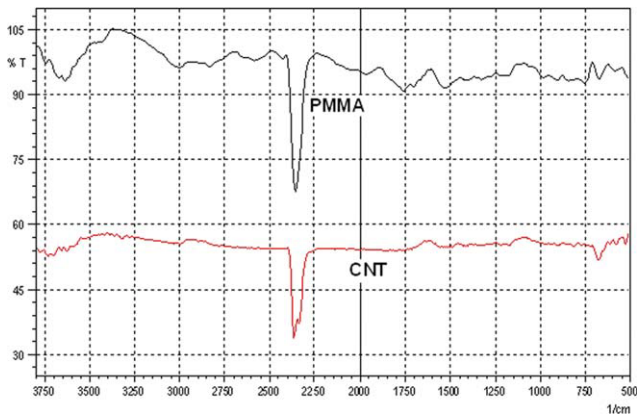

Figure 5 IR spectra of PMMA polymer and CNT. [Color figure can be viewed in the online issue, which is available at wileyonlinelibrary.com.]

groups in functionalized MWCNTs interact with CO— group of PMMA.[18–20] The peak is sharper for *ex situ* composites. The IR spectrum shows that the intensity of peak for C=O stretching of the carboxylic acid (at 1720 cm^{-1}) became weaker after the coupling for *ex situ* composites than the *in situ* one (Fig. 6). Therefore, from the different IR spectra it is evident that the mode of chemical reaction between resin and MWCNT is different. However, there are few literatures regarding the π-bond attack of CNT by radicals.[21–24] Jia et al.[22] and Park et al.[24] studied PMMA/CNT composites and concluded that CNTs take part in the MMA polymerization and that a strong binding interface is formed between PMMA and CNTs. They speculated that the FT-IR peak at around 1660 cm^{-1} might result from a CC bond between CNT and PMMA. In this study, a peak at 1663 cm^{-1} is also present for *in situ* composites. However, this may be controversial because of the interference with the alkane chain backbone of common polymers. These facts demonstrate that for *in situ* composites multiwall nanotubes (MWNT) participate in the MMA polymerization via the carbon–carbon double bond whereas incase of *ex situ* technique this probably by H-bonding through —COOH group and PMMA polymer. Meng et al. have prepared PMMA-functionalized carboxyl MWCNT using carboxylate CNT and MMA as reactants and benzoyl peroxide as an initiator agent by an *in situ* polymerization process. The functionalized MWCNT were characterized using transmission electron microscope, scanning electron microscope, nuclear magnetic resonance, FTIR, TGA, and Raman. The results indicate that the PMMA chains are covalently linked with the surface of carboxylate CNT.[25]

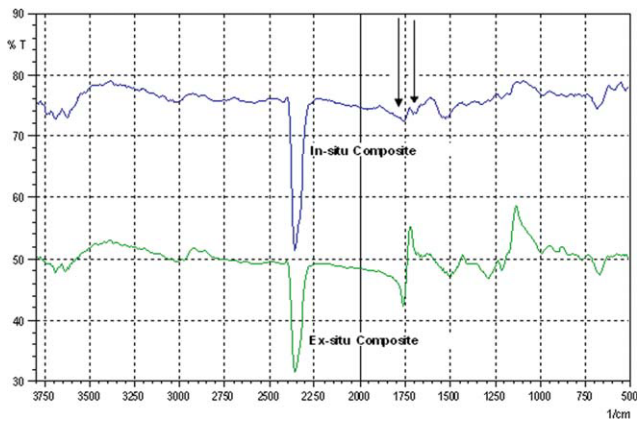

Figure 6 IR spectra of PMMA composite reinforced with CNT by *in situ* and *ex situ* techniques. [Color figure can be viewed in the online issue, which is available at wileyonlinelibrary.com.]

Degree of conversion by IR study

The degree of conversion (DC) (%) of monomer-to-polymer under investigation was calculated by FT-IR spectroscopy and by comparing the absorbance ratio using a standard baseline technique of the C=C peak from the methacrylate group at 1640 cm^{-1} to that of the unchanging C=O peak from the ester group at 1720 cm^{-1}. The latter was used as a reference peak, before (monomer) and after polymerization (group C), and after the two postpolymerization treatments (groups Multi wall and West Bengal). By taking the ratio between the two absorbances, the fraction of unreacted double bonds could be calculated from the formula:[26,27]

$$DC\% = 1 - \left\{ \frac{[Abs(C{=}C)/Abs(C{=}O)]_{Polymer}}{[Abs(C{=}C)/Abs(C{=}O)]_{Monomer}} \right\} \times 100\%$$

Regardless of the spectral region to be used, determination of DC is facilitated when the material presents a stable absorption band, whose intensity is unaltered during polymerization process. This band is used as an internal standard of normalization. In this case, it is unnecessary to account the sample thickness.

Calculation for DC% is shown in Table I and the values are: DC for *in situ* composites = 31.7%, for PMMA (commercial) = 33.8%. It indicates that the conversion in both the cases is quite comparable.

TABLE I
IR Peak and Absorption Used to Calculate Degree of Conversion

Polymer	1639.38 cm^{-1}	1720.39 cm^{-1}	Degree of conversion
Monomer	0.06	0.07	
PMMA	0.0762	0.0758	33.8%
Insitu composites	0.1190	0.1192	31.7%

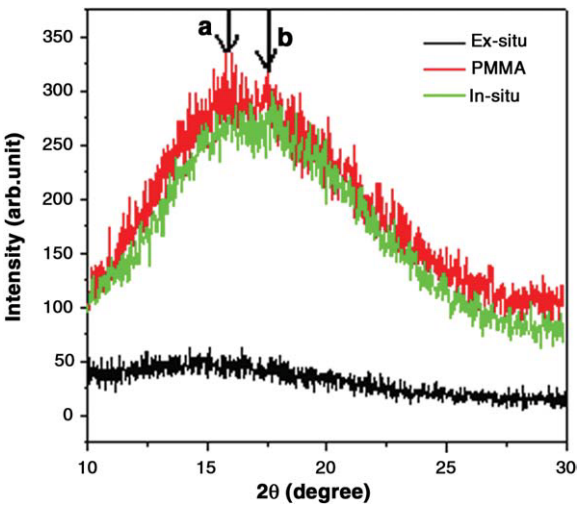

Figure 7 XRD patterns of PMMA and PMMA composites reinforced with CNT by *in situ* and *ex situ* techniques. [Color figure can be viewed in the online issue, which is available at wileyonlinelibrary.com.]

XRD study

XRD patterns of PMMA and both *in situ* and *ex situ* composites are presented in Figure 7. Basically PMMA shows broad peak (in the marked region where a: $2\theta = 15.96$ and b: $2\theta = 17.5$, which is typical of this amorphous polymers. The *in situ* nanocomposite exhibits similar type of XRD pattern indicating that probably due to the presence of —COOH group, the MWCNT became incorporated into the polymer chain during polymerization forming a kind of chemically linked short-term branched copolymer. As a result, the resultant nanocomposite produced XRD, which has more or less similar features of neat PMMA. The degree of amorphousness is extreme with the *ex situ* nanocomposite indicating a different chemical structure. Obviously, the *ex situ* reinforcement has resulted in total destructive interference of the reflected X-rays indicating a) absence of even the smallest amount of long range order, and/or b) the X-rays may have been diffracted randomly by the CNT molecules without penetrating the polymer chains. This needs to be studied in further details.

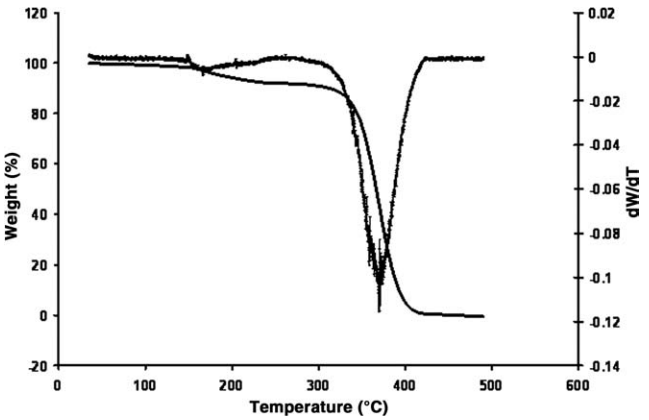

Figure 9 TGA/DTG curve for PMMA composites reinforced with CNT by *in situ* technique.

Traces of TGA of PMMA, *in situ* and *ex situ* composites are shown in Figures 8–10. From Table II it is clear that PMMA shows three stages of degradation—the first is due to decomposition of relatively week head-to-head linkage, impurities, and solvent in the lattices. The second is the chain end of PMMA, and the third is the PMMA main chains decomposition. The three steps of pure PMMA are at 168, 224, and 372°C. The TGA curves for PMMA-MWCNT *in situ* and *ex situ* composites also seem to be three-step decomposition reaction (Fig. 11). The amount of degradation at the second step due to chain end decomposition is increased to a greater extent compared with PMMA and the *ex situ* composite. It may be attributed to the incorporation of MWCNT in main polymerization reaction through its double bond as explained by the IR study. As a result, the amount of main chains decomposition of the *in situ* composite is lower than that of pure PMMA and the *ex situ* composite. From Table II, it is evident that the maximum degradation temperature

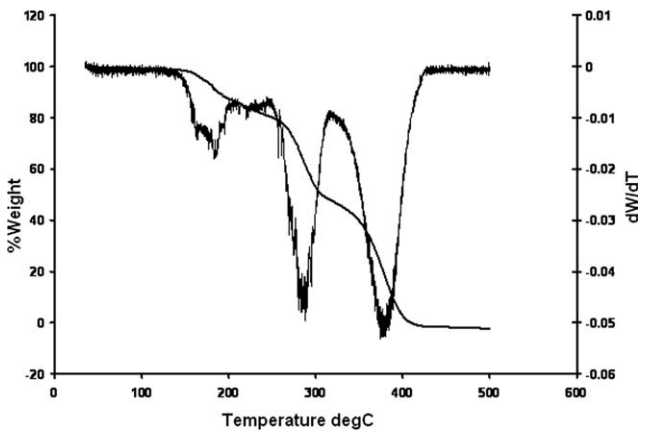

Figure 8 TGA/DTG curve for PMMA polymer.

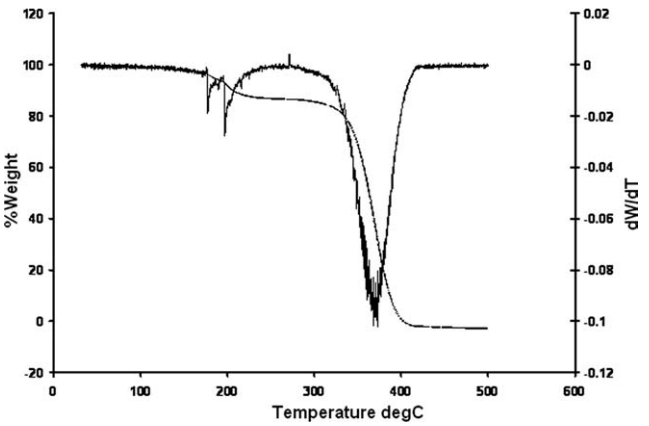

Figure 10 TGA/DTG curve for PMMA composites reinforced with CNT by *ex situ* technique.

TABLE II
TGA Data for PMMA Carbaon Nano Tube Composites

Sample	No. of transition	Initial temperature (°C)	Final temperature (°C)	Degradation peak temperature (°C)	Degradation at corresponding transition (%)	% weight residue
PMMA	1	145	209	168	7.95	Nil
	2	209	277	224	3.25	
	3	277	427	372	88.80	
Insitu composite	1	142	207	186	15.7	Nil
	2	207	317	283	36	
	3	317	431	383	50.3	
Ex situ composite	1	140	195	177	9.25	Nil
	2	195	236	197	4.7	
	3	236	423	372	87.05	

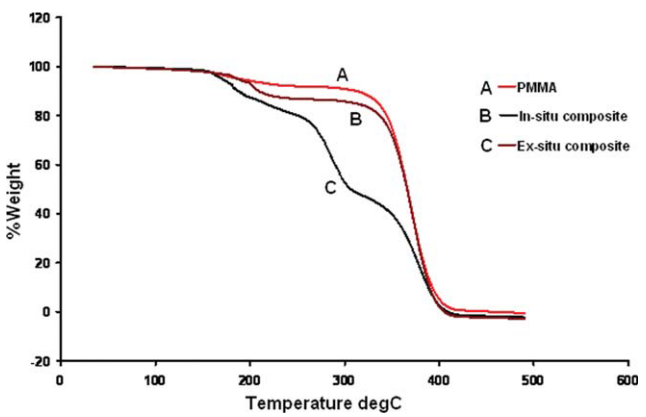

Figure 11 TGA curves of PMMA and PMMA composites reinforced with CNT by *in situ* and *ex situ* techniques. [Color figure can be viewed in the online issue, which is available at wileyonlinelibrary.com.]

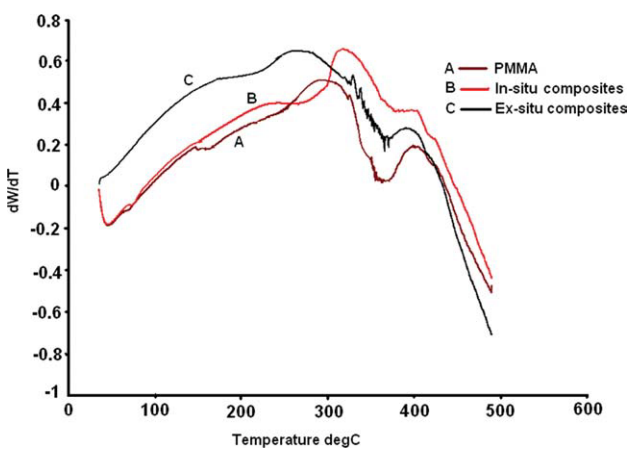

Figure 12 DTA curves for PMMA and PMMA composites reinforced with CNT by *in situ* and *ex situ* techniques. [Color figure can be viewed in the online issue, which is available at wileyonlinelibrary.com.]

has been shifted to higher region for *in situ* composites compared with PMMA itself and the *ex situ* composites indicate better thermal stability. No residue has been found at the end of degradation for all samples.

From the DTA curve (Fig. 12) of all the samples it was observed that there are two endothermic peaks occurring around 150–280°C and one exothermic peak at 323°C. For PMMA, endothermic peak was observed in the DTA curve at 165°C, which is characteristic of high molecular weight PMMA and is believed to be due to disentanglements of the high molecular weight chains.[3] A small second endothermic peak also associated along with the first may be due to the relaxation phenomena. The exothermic peak is probably due to the random bond scission of the polymer chains. The three peaks are present at more or less similar region for *ex situ* composites whereas they have been shifted toward higher region for *in situ* composites indicating better thermal stability. Incorporation of CNT to the main chain through its double bond imparts better thermal stability. Thermal study of amide functionalized SWNT/PMMA nanocomposites by Ramanathan et al.[28] showed a significant shift of the weight loss toward higher temperature for both unmodified and amide-functionalized SWNT/PMMA composites, with stabilization 50°C higher than that for the neat polymer. The improved thermal stability of SWNT/PMMA composites is quite likely associated with the interaction between polymer and SWNTs.

CONCLUSIONS

a. Incorporation of —COOH functionalized MWCNT in main chain of PMMA polymer does not improve all the properties to similar extent.
b. Incorporation of —COOH functionalized MWCNT in main chain of PMMA does not modify the resistivity or XRD peak of PMMA polymer but

affects thermal properties to a smaller extent. But the resistivity modification of PMMA by *ex situ* incorporation technique of MWNT imparts semiconducting nature to the total insulating PMMA.

c. Functionalization along with the used *ex situ* and *in situ* technique to improve the electrical conductivity of a totally insulating polymer PMMA. Chang et al.[29] fabricated composite using polyacrylonitrile nanofibres as a scaffold of MWNTs, and PMMA as the macroscopic polymer matrix by combining electrospinning and *in situ* polymerization.
d. However, there are scopes to judge other properties of the composites in future investigation. Depending on needs, then we can successfully use the suitable technique to modify PMMA.

References

1. Blond, D.; Barron, V.; Ruether, M.; Ryan, K. P.; Nicolosi, V.; Blau, W. J.; Coleman, J. N. Adv Funct Mater 2006, 16, 1608.
2. Park, J. H.; Alegaonkar, P. S.; Jeon, S. Y.; Yoo, J. B. Comp Sci Tech 2008, 68, 753.
3. Cheng Ma, P.; Jang-Kyo, K.; Ben Zhong, T. Comp Sci Tech 2007, 67, 2965.
4. Luo, D.; Wang, W.; Takao, Y. Comp Sci Tech 2007, 67, 2947.
5. Costache, M. C.; Wang, D.; Heidecker, M. J.; Manias, E.; Wilkie, C. A. Polym Adv Technol 2006, 17, 272.
6. Yuen, S.; Ma, C. M.; Chuang, C.; Yu, K.; Wu, S.; Yang, C.; Wei, M. Comp Sci Tech 2008, 68, 963.
7. Du, F.; Fisher, J.; Winey, K. J Polym Sci B Polym Phys 2003, 41, 3333.
8. Ivanov, I. N.; Puretzky, A. A.; Lance, M. J.; Jesse, S.; Viswanathan, S.; Britt, P. F.; Geohegan, D. B. Presented at American Physical Society, Annual APS March Meeting 2003, March 3–7 2003, abstract #W26.006.
9. Sundaray, B.; Subramanian, V.; Natarajan, T. S.; Krishnamurthy, K. Appl Phys Lett 2006, 88, 143114.
10. Kathyayini, H.; Willems, I.; Fonseca, A.; Nagy, J. B.; Nagaraju, N. Catal Commun 2006, 7, 140.
11. Ham, H. T.; Choi, Y. S.; Jeong, N.; Chung, I. J Polym 2005, 46, 6308.
12. Ham, H. T.; Choi, Y. S.; Chee, M. G.; Chung, I. J. J Polym Sci A Polym Chem 2006, 44, 573.
13. Chern, C. S.; Tang, H. J. J Appl Polym Sci 2005, 97, 2005.
14. Yao, Z. L.; Braidy, N.; Botton, G. A.; Adronov, A. J Am Chem Soc 2003, 25, 16015.
15. Banerjee, S.; Hemraj-Benny, T.; Wong, S. S. Adv Mater 2005, 17, 17.
16. Tasis, D.; Tagmatarchis, N.; Georgakilas, V.; Prato, M. Chem-Eur J 2003, 9, 4001.
17. Luechinger, N. A.; Booth, N.; Heness, G.; Bandyopadhyay, S.; Grass, R. N.; Stark, W. J Adv Mater 2008, 20, 3044.
18. Velasco-Santos, C.; Martıñez-Hernańdez, A. L.; Fisher, F. T.; Ruoff, R.; Castano, V. M. Chem Mater 2003, 15, 4470.
19. Velasco-Santos, C.; Martıñez-Hernańdez, A. L.; Lozada-Cassou, M.; Alvarez-Castillo, A.; Castano, V. M. Nanotechnology 2002, 13, 495.
20. Zhang, J. M.; Zhang, D. H.; Shen, D. Y. Macromolecules 2002, 35, 5140.
21. Chen, R. J.; Zhang, Y.; Wang, D.; Dai, H. J Am Chem Soc 2001, 123, 3838.
22. Jia, Z.; Wang Z. Xu, C.; Liang, J.; Wei, B., Wu, D., Zhu, S. Mater Sci Eng A 1999, 271, 395.
23. Mitchell, C. A.; Bahr, J. L.; Arepalli, S.; Tour, J. M.; Krishnamoorti, R. Macromolecules 2002, 35, 8825.
24. Park, S. J.; Cho, M. S.; Lim, S. T.; Choi, H. J.; Jhon, M. S. Macromol Rapid Commun 2003, 24, 1070.
25. Meng, Q.; Zhang, X.; Bai, S.; Wang, X. Chin J Chem Phys 2007, 20, 660.
26. Urbana, V. M.; Machadoa, A. L.; Eduardo, V. C.; Jorgea, É. G.; Santosb, L. P. S.; Leiteb, E. R.; Canevaroloc, S. V. Mater Res 2007, 10, 191.
27. Moraes L. G. P.; Rocha R. S. F.; Menegazzo L. M.; Araújo E. B. D.; Yukimitu K.; Moraes J. C. S. J Appl Oral Sci 2008, 16, 145.
28. Ramanathan, T.; Liu, H.; Brinson, L. C. J Polym Sci B Polym Phys 2005, 43, 2269.
29. Chang, Z. J.; Zhao, X., Zhang, Q. H.; Chen, D. J. Polym Lett 2010, 4, 47.